Production and characterization of recombinant human lactoferrin

Veen, H.A. van

Chapter 6

The protein structure of recombinant human lactoferrin produced in the milk of transgenic cows closely matches the structure of human milk-derived lactoferrin★

Ellen A. J. Thomassen[1,‡], Harrie A. van Veen[2,*,‡], Patrick H. C. van Berkel[2,3], Jan H. Nuijens[2] & Jan Pieter Abrahams[1]

[1]*Biophysical Structural Chemistry, Leiden Institute of Chemistry, Leiden University, Einsteinweg 55, 2333 CC Leiden, The Netherlands*
[2]*Pharming, Archimedesweg 4, 2333 CN Leiden, The Netherlands*
[3]*Current address: Genmab, Yalelaan 60, 3584 CM, Utrecht, The Netherlands*

Received 1 November 2004; accepted 27 February 2005

Key words: iron-binding, lactoferrin, transgenic cows

Abstract

Human lactoferrin (hLF) is an iron-binding glycoprotein involved in the host defence against infection and excessive inflammation. As the availability of (human milk-derived) natural hLF is limited, alternative means of production of this biopharmaceutical are extensively researched. Here we report the crystal structure of recombinant hLF (rhLF) expressed in the milk of transgenic cows at a resolution of 2.4 Å. To our knowledge, the first reported structure of a recombinant protein produced in milk of transgenic livestock. Even though rhLF contains oligomannose- and hybrid-type N-linked glycans next to complex-type glycans, which are the only glycans found on natural hLF, the structures are identical within the experimental error (r.m.s. deviation of only 0.28 Å for the main-chain atoms). Of the differences in polymorphic amino acids between the natural and rhLF variant used, only the side-chain of Asp^{561} could be modeled into the rhLF electron density map. Taken together, the results confirm the structural integrity of the rhLF variant used in this study. It also confirms the validity of the transgenic cow mammary gland as a vehicle to produce recombinant human proteins.

Abbreviations: LF – lactoferrin; hLF – human lactoferrin; natural hLF – hLF purified from human milk; rhLF – recombinant hLF; iron-saturated rhLF – rhLF that has been completely saturated with iron *in vitro*

Introduction

Lactoferrin (LF) is a metal-binding glycoprotein of 77 kDa belonging to the transferrin family (Anderson et al., 1989). The molecule is found in milk, tears, saliva, bronchial, intestinal and other secretions, but also in the secondary granules of neutrophils (Nuijens et al., 1996). Based on the many reports of its antimicrobial and anti-inflammatory activity in vitro, LF is thought to be involved in the host defense against infection and excessive inflammation, most notably at mucosal surfaces (Nuijens et al., 1996). Antimi-

*Author for correspondence
E-mail: h.veen@pharming.com
‡These authors have contributed equally to this paper.
★The PDB-code of recombinant human lactoferrin is 2BJJ

crobial activities of LF include bacteriostasis by the sequestration of free iron (Reiter et al., 1975) and bactericidal activity by destabilization of the cell-wall (Ellison III et al., 1988; Ellison III & Giehl, 1991). Anti-inflammatory actions of LF include inhibition of hydroxyl-radical formation (Sanchez et al., 1992), of complement activation (Kijlstra & Jeurissen, 1982) and of cytokine production (Zucali et al., 1989) as well as neutralization of lipopolysaccharide (LPS) (Lee et al., 1998). Due to these biological activities of LF, a wide variety of applications in human health care has been proposed, such as treatment of infectious and inflammatory diseases. As a nutraceutical application, the molecule can be used as a component of clinical nutrition products aimed at the prevention and treatment of gastrointestinal tract infections and inflammations.

The DNA and amino acid sequences of human lactoferrin (hLF) have been determined (Metz-Boutigue et al., 1984; Rey et al., 1990). Human LF consists of a polypeptide chain of 692 amino acids, which is folded into two globular lobes (Anderson et al., 1989). These lobes, designated the N- and C-lobe, share an internal amino acid identity of about 40% (Metz-Boutigue et al., 1984) and are connected by a α-helix. Each lobe folds into α-helix and β-sheet arrays to form domains I and II, respectively, which are connected by a hinge region, creating a deep iron-binding cleft within each lobe. Each cleft binds a single ferric ion with high affinity while simultaneously incorporating a bicarbonate ion (Anderson et al., 1989). Crystallographic studies of hLF have showed that upon binding of iron, domain I of the N- and C-lobe rotates relative to domain II by ~54° and ~20°, respectively, resulting in a more globular closed, and stable conformation of the entire molecule (Baker et al., 2000). Next to the high affinity metal binding in the iron-binding cleft, LF also binds metals with much lower affinity (Nagasako et al., 1993). This occurs at least in part via surface-exposed histidyl residues (Hutchens & Yip, 1991). Whereas some of the biological activities of hLF relate to high or low affinity iron-binding, others are mediated by a positively charged domain located in the N-terminus. This domain binds to negatively charged ligands such as the lipid A portion of LPS (Appelmelk et al., 1994), DNA (He & Furmanski, 1995), heparin (Mann et al., 1994) as well as other proteins such as lysozyme (van Berkel et al., 1995) and specific receptors (Ziere et al., 1993; Legrand et al., 1997).

Human LF contains three possible N-glycosylation sites, Asn^{138} in the N-lobe and Asn^{479} as well as Asn^{624} in the C-lobe (Rey et al., 1990), which are utilized in about 94, 100 and 9% of the molecules, respectively (van Berkel et al., 1996).

Recently, the production of recombinant hLF (rhLF) in the milk of transgenic cows was reported (van Berkel et al., 2002). Comparative studies between rhLF and hLF from human milk (natural hLF) revealed identical iron-binding and release properties, and despite differences in N-linked glycosylation, equal effectiveness in various infection models (van Berkel et al., 2002). Here, we report the crystallographic structure of rhLF in its iron-saturated conformation. The structure appeared to be almost identical to the structure reported for iron-saturated natural hLF (Haridas et al., 1995).

Materials and methods

Expression and purification of rhLF

The production and purification of rhLF from the milk of transgenic cows has been described previously (van Berkel et al., 2002). Briefly, a genomic hLF sequence with polymorphic amino acids at position 4 (insertion of Arg), 11 (Ala), 29 (Arg) and 561 (Asp) (van Veen et al., 2004) under control of regulatory elements from the bovine αS_1 casein gene, was introduced into the bovine germline. The resulting transgenic cattle lines showed rhLF expression levels between 0.4 and 2.5 g/L. Purified rhLF was saturated with iron as described (van Berkel et al., 1995).

Crystallization

Crystals were grown by micro-dialysis of rhLF (54 mg/ml in 0.9% NaCl) in a 100 μl dialysis button against 5 mM sodium phosphate pH 8.5 with 10% (v/v) ethanol at 4°C. Deep red crystals appeared after 4 weeks and grew to dimensions of approximately $3 \times 2 \times 1$ mm^3. The protein crystallized in the orthorhombic space-group $P2_12_12_1$, with cell dimensions $a = 55.94$, $b = 97.38$, and $c = 156.30$ Å with 1 molecule in the asymmetric unit.

Data collection

The dialysis button was transferred to 5 mM sodium phosphate pH 8.5 complemented with 20% (v/v) 2-methyl-2,4-pentanediol (MPD) for a week at 4°C to stabilize the crystals, as described (Anderson et al., 1989). Part of a crystal was broken off and mounted in a quartz capillary. X-ray data were collected at room temperature on a FR591 rotating-anode generator equipped with a MAR345 image-plate detector, using Cu Kα radiation ($\lambda = 1.5418$ Å). The crystal-to-detector distance was 220 mm and a 0.5° oscillation angle was used per image for a total of 369 images. The intensities were indexed with MOSFLM (Leslie, 1999) and scaled using SCALA (Evans, 1993). During the scaling process it was observed that a number of the images were not useful, which is most likely caused by a non-uniform quality of the crystal in different directions. These images were left out of the scaling process and not used any further. The resulting data set contained 154 images (77°) and 104905 reflections of which 33492 were unique. The overall completeness of the data set was 96.2%, with a completeness of 97.9% in the highest resolution bin (2.53–2.40 Å). The overall redundancy and R_{sym} were 3.3 and 0.057, respectively. Data collection and processing details are summarized in Table 1.

Table 1. Data-collection and processing parameters

Data collection	rhLF expressed in bovine milk
Crystal dimensions (mm^3)	$3 \times 2 \times 1$
Wavelength (Å)	1.5418
Resolution range (Å)	81.65–2.40
Crystal system	orthorhombic
Space group	$P2_12_12_1$
Unit cell parameters (Å)	$a = 55.94$, $b = 97.38$, $c = 156.30$
Total number of reflections	104905
Number of unique reflections	33492
Multiplicity	3.3 (3.3)[a]
Rsym[b]	0.057 (0.33)
Completeness (%)	96.2 (97.9)
Average I/σ(I)	8.9 (2.2)
Solvent content (%)	55.51
V_M ($Å^3$/Da)	2.8

[a]Data statistics of the outer resolution shell (2.53–2.40 Å) are given in parentheses, where applicable.
[b]$R_{sym} = \Sigma_h \Sigma_i |I_{hi} - \langle I_h \rangle| / \Sigma_h \Sigma_i |I_{hi}|$, where I_{hi} is the intensity of the ith measurement of the same reflection and $\langle I_h \rangle$ is the mean observed intensity for that reflection.

Structure elucidation and refinement

The structure was determined by molecular replacement, using MOLREP (Vagin & Teplyakov, 1997) and the structure of iron-saturated natural hLF (Haridas et al., 1995) as the search model. The search model included two Fe^{3+} and two CO_3^{2-} ions, but all waters and carbohydrates were omitted. The rotation and translation functions were determined and the best solution had an R-factor of 0.294 and a correlation coefficient of 0.814. Instead of a full molecular replacement, a rigid body refinement could have been performed, after applying an anti-clockwise rotation parallel to the b-axis on the search model, changing a into c and c into $-a$, which would have given the same result. The model was refined using restrained refinement using REFMAC (Murshudov et al., 1997) using 30833 reflections in the resolution range 19.63–2.40 Å (for the refinement statistics see Table 2). Water molecules were built using ARP (Lamzin & Wilson, 1997). Electron density maps were calculated and carbohydrates were fitted into the $2F_o–F_c$ electron density. The final model was checked using

Table 2. Refinement statistics

Refinement	rhLF expressed in bovine milk
Resolution range (Å)	19.63–2.40
Number of reflections	30833 (1640)[a]
Rfactor[b]	0.18 (0.23)
Protein atoms/waters	5365/54
r.m.s. deviations bonds (Å)	0.013
r.m.s. deviations angles (°)	1.40
Average B value: protein/solvent ($Å^2$)	50.27/39.60
Average B value: sugar/Fe^{3+}/CO_3^{2-} ($Å^2$)	86.29/31.90/26.43
Ramachandran statistics[c] (%)	86.4/13.0/0.3/0.3

[a]Data statistics of Rfree are given in parentheses, where applicable.
[b]$R = \sum||F_{obs}(hkl)| - |F_{calc}(hkl)|| / \sum |F_{obs}(hkl)|$.
[c]According to the program PROCHECK (Laskowski et al., 1993). The percentages are indicated of residues in the most favoured, additionally allowed, generously allowed and disallowed regions of the Ramachandran plot, respectively.

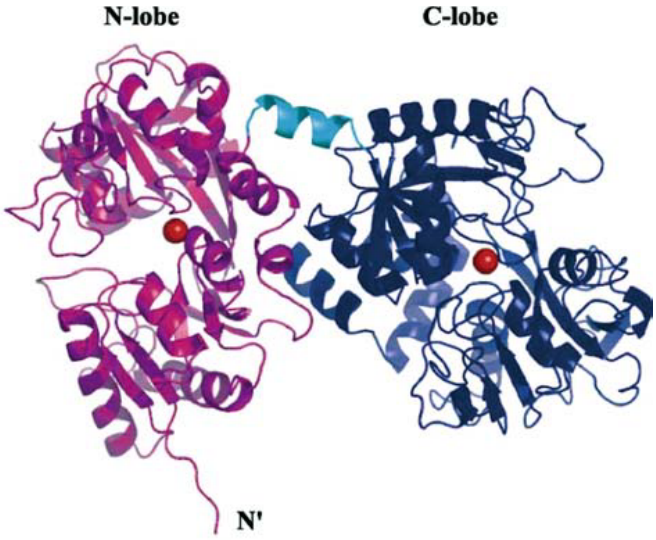

Figure 1. Ribbon diagram of rhLF expressed in the milk of transgenic cows. The N-lobe (residue 1–334) is shown in magenta and the C-lobe (residue 346–692) is shown in dark blue. The α-helix connecting the two lobes is depicted in light blue (residue 335–345). Red spheres show the iron atoms. The figure was prepared with PyMOL (DeLano, 2002).

PROCHECK (Laskowski et al., 1993) and WHATIF (Vriend, 1990).

Structural comparisons

The structure of rhLF isolated from transgenic bovine milk was compared to the structure of iron-saturated natural hLF (PDB-code 1LFG, Haridas et al., 1995), using LSQKAB from the CCP4 program suite (CCP4 suite, 1994). The amino acid residues 1–4 and 1–5 from natural hLF and rhLF, respectively, were disordered and therefore left out of the calculations.

Table 3. Iron site geometry in the N- and C-lobe of rhLF

N-lobe*		C-lobe#	
Atoms	Bond length (Å)	Atoms	Bond length (Å)
Fe–O^{61}	2.22	Fe–O^{396}	2.10
Fe–O^{93}	1.90	Fe–O^{436}	1.95
Fe–O^{193}	1.88	Fe–O^{529}	1.87
Fe–N^{254}	2.21	Fe–N^{598}	2.36
Fe–O1	2.18	Fe–O1	2.05
Fe–O2	2.24	Fe–O2	2.27

*The ligand atoms in the N-lobe: Asp^{61} OD1, Tyr^{93} OH, Tyr^{193} OH, His^{254} Nε2, carbonate atoms, O1 and O2.
#The ligand atoms in the C-lobe: Asp^{396} OD1, Tyr^{436} OH, Tyr^{529} OH, His^{598} Nε2, carbonate atoms O1 and O2. The bond lengths are from refinement using Refmac (Murshudov et al., 1997).

Results and discussion

rhLF model

The crystallographic structure of iron-saturated rhLF from transgenic bovine milk refined at 2.4 Å (Figure 1) shows clearly the bilobal structure of hLF with each lobe divided into the two domains and the iron atoms buried in the interdomain clefts. The final model consists of 692 amino acid residues, 54 water molecules, two Fe^{3+} ions, two CO_3^{2-} ions, and two *N*-acetylglucosamine residues that are N-linked to Asn^{138} and Asn^{479} (numbering according to Rey et al., 1990). The model has an R-factor of 0.18 and an Rfree of

Table 4. Anion hydrogen bonding distances in the two lobes of rhLF

N-lobe		C-lobe	
Hydrogen bonds	Bond length (Å)	Hydrogen bonds	Bond length (Å)
O1–N^{124}	2.72	O1–N^{468}	2.83
O2–NE^{122}	2.81	O2–NE^{466}	2.76
O2–$NH2^{122}$	2.88	O2–$NH2^{466}$	2.84
O3–N^{125}	3.09	O3–N^{469}	2.92
O3–$OG1^{118}$	2.56	O3–$OG1^{462}$	2.75

The carbonate atoms O1, O2 and O3. The bond lengths are measured in Xfit (McRee, 1999).

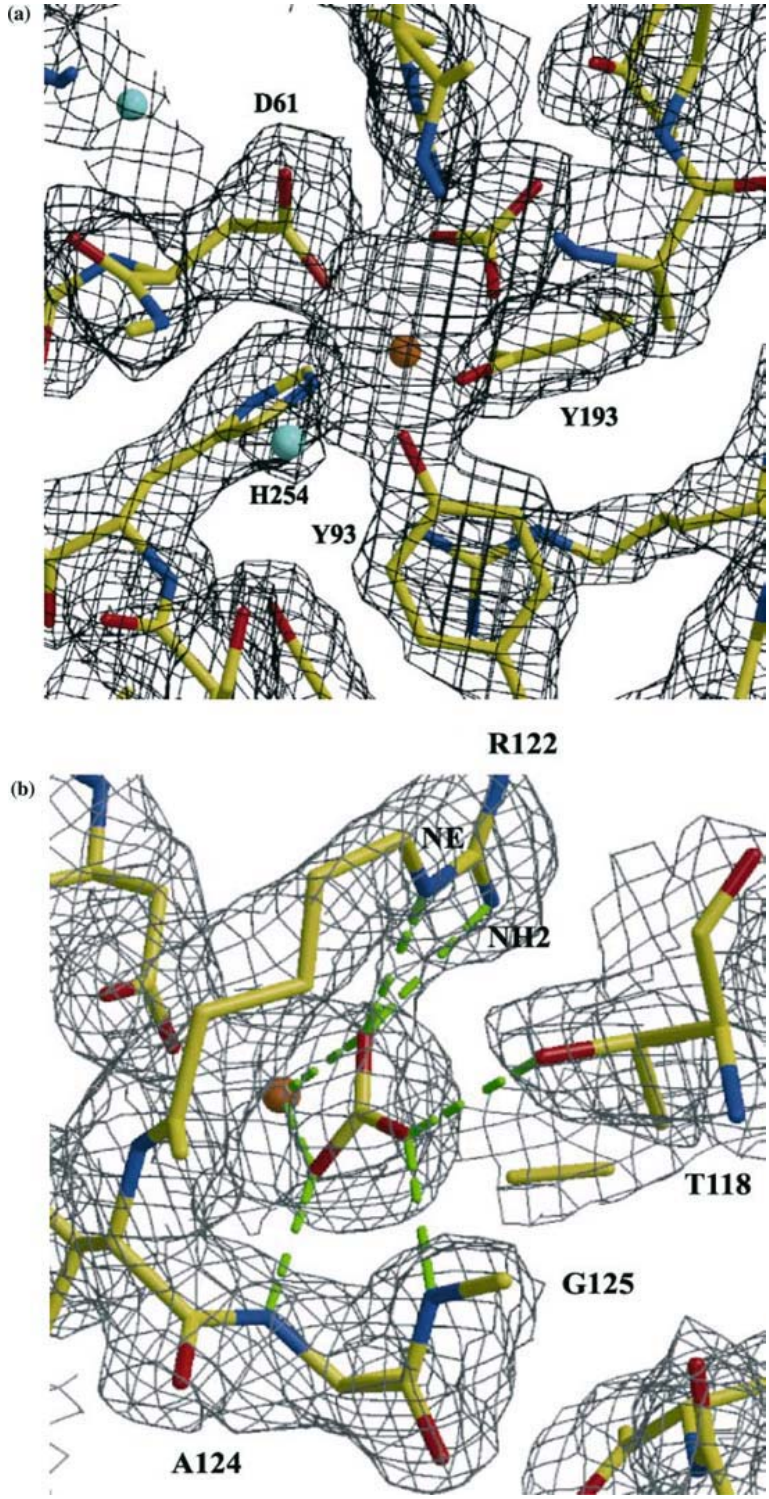

Figure 2. (a) Crystallographic electron density surrounding the ferric ion in the N-lobe of rhLF. The iron binding residues Tyr^{93}, Tyr^{193}, Asp^{61}, His^{254} and carbonate^{695} are shown in ball-and-stick representation surrounded by the final $2F_o–F_c$ electron density map contoured at 1.5σ. A red sphere indicates the iron atom and blue spheres indicate waters. 2. (b) Crystallographic electron density surrounding the anion binding site in the N-lobe of rhLF. The anion binding residues Thr^{118}, Arg^{122}, Ala^{124} and Gly^{125} are shown in ball-and-stick representation surrounded by the final $2F_o–F_c$ electron density map contoured at 1.5σ. A red sphere shows the iron^{693}. The pictures were created with Xtalview (McRee, 1999).

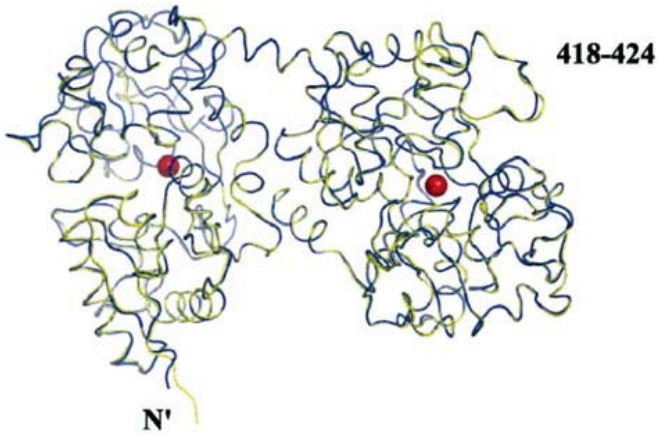

Figure 3. Cα superposition of rhLF and natural hLF. rhLF expressed in bovine milk is shown in yellow and natural hLF isolated from human milk in blue. Red spheres show the iron atoms. The figure was prepared with PyMOL (DeLano, 2002).

0.23. The Ramachandran statistics (Table 2) show 86.4% of the residues to be in the "most favored" regions and 13.3% in the "allowed" regions; only 0.3% is in the "disallowed" region, which are residues Leu^{300} and Leu^{643}. As described before (Haridas et al., 1995), both residues are present in a γ-turn, which seems to be a conserved property of all transferrin structures determined. The N-terminal amino acid stretch (Gly^1-Arg^2-Arg^3-Arg^4-Arg^5-) was disordered and could not be modeled. Also the flexible surface loop at residues 418–424 showed no ordered density at 1σ, but at 0.7σ the main-chain and most of the side-chain atoms became visible. The observed disorder and/or flexibility of these two regions is consistent with described previously (Haridas et al., 1995; Sun et al., 1999) and may be explained by lacking of protein interactions. Many of the amino acid residues that are exposed to solvent have disordered side-chains, especially the long side-chains of arginine and lysine residues, and have corresponding high B factors.

Iron and anion binding of rhLF

The structure of rhLF isolated from the milk of transgenic cows was determined in its iron-saturated conformation. As some biological actions of hLF depend on the high-affinity binding of iron, the positions of the ferric ions and anions in the model were closely evaluated. Figure 2a and b show the electron densities surrounding the ferric and carbonate ion, respectively, in the N-lobe of rhLF. The ferric ion is coordinated by Asp^{61}, Tyr^{93}, Tyr^{193}, His^{254} and the carbonate ion, which is identical as previous described for iron-saturated natural hLF from human milk (Haridas et al., 1995). In addition, the metal to ligand bond lengths are all close to 2.0 Å (Table 3), which is as expected for coordination of the ferric ion (Haridas et al., 1995). The coordination of the carbonate ion by Thr^{118}, Arg^{122}, Ala^{124} and Gly^{125} and hydrogen bonding distances of about 3 Å (Figure 2b, Table 4) also matches with previous reported for natural hLF. The results for the position of the ferric and carbonate ion in the C-lobe of rhLF (Tables 3 and 4) are similar to observed for the N-lobe at least within the accuracy of the present X-ray analysis. Taken together, the coordination and bonding distances of the ferric and carbonate ion in the two lobes of rhLF are equal within the experimental error compared to iron-saturated natural hLF.

Comparison of rhLF and natural hLF

The folding of rhLF is the same as that for natural hLF isolated from human milk (1LFG). The structure of rhLF was superimposed on natural hLF, the r.m.s. deviation in the atomic positions of the main-chain atoms is 0.28 Å, omitting the disordered N-terminus. The superimposed structures are shown in Figure 3, only amino acid residues 418–424 which are in a flexible loop and therefore may adopt alternative conformations and the N-terminus which is completely disordered show differences between residues from rhLF and natural hLF. Most of the amino acid

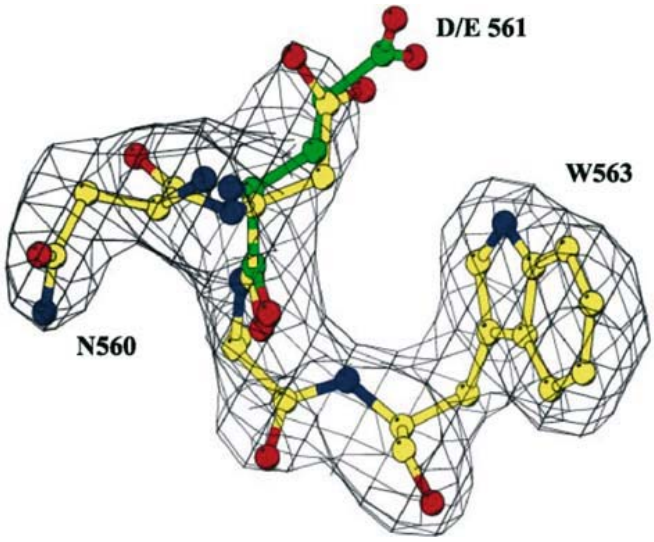

Figure 4. Crystallographic electron density surrounding Asp^{561}. rhLF amino acid residues Asn^{560}, Asp^{561}, Ala^{562}, and Trp^{563} are shown in ball-and-stick representation with carbon atoms in yellow, surrounded by the final $2F_o–F_c$ electron density map contoured at 1σ. At the polymorphic position 561 (numbering according to rhLF) the glutamatic acid (E) is shown in ball-and-stick representation with carbon atoms in green. Picture was prepared with BOBSCRIPT (Esnouf, 1999), which is based on MOLSCRIPT (Kraulis, 1991).

side-chains in both structures have similar orientations except for the regions that are disordered or flexible such as the N-terminus, the loop spanning amino acids 418–424 and solvent exposed residues. Previously, polymorphic sites in the hLF coding sequence were reported at amino acid position 4 (deletion of Arg), position 11 (Ala or Thr), position 29 (Arg or Lys) and position 561 (Asp or Glu) (van Veen et al., 2004). Differences in polymorphic sites between rhLF and the natural hLF variant described by Haridas et al. (1995) are at position 4 (- → Arg), 29 (Lys → Arg) and 561 (Glu → Asp). The Arg^4 residue of rhLF could not be modeled, the N-terminal stretch Gly^1-Arg^2-Arg^3-Arg^4-Arg^5 may however be modeled upon binding of heparin, as Arg^2-Arg^3-Arg^4-Arg^5 is part of the positively charged domain responsible for binding of the ligand (Mann et al., 1994). The side chain of the solvent-exposed Arg^{29} residue was disordered and could not be modeled. Figure 4 shows the polymorphic site Asp^{561} in the $2F_o–F_c$ density map. The polymorphic sites did neither change the structure of rhLF nor its biochemical activity, when compared to natural hLF (van Berkel et al., 2002).

Glycosylation

Human lactoferrin contains three possible N-glycosylation sites, Asn^{138} in the N-lobe and Asn^{479} as well as Asn^{624} in the C-lobe (Rey et al., 1990), which are utilized in about 94, 100 and 9% of the molecules, respectively (van Berkel et al., 1996). The glycans of natural hLF are of the sialyl-*N*-acetyllactosaminic type (Spik et al., 1982). Previously, reported was that rhLF from transgenic bovine milk also contains oligomannose and/or hybrid-type glycans (van Berkel et al., 2002).

In the rhLF structure described here, interpretable density for single carbohydrates was present at glycosylation sites Asn^{138} and Asn^{479}. The two *N*-acetylglucosamine residues were built into the $2F_o–F_c$ density map contoured at 0.9σ. The *N*-acetylglucosamine at position Asn^{479} is shown in Figure 5. Further carbohydrates were insufficiently ordered to extend the model.

Conclusions

The application of rhLF from bovine milk in human health care requires a thorough comparison of the physico-chemical and biological characteristics of the recombinant with the natural form. Here we report that despite the presence of polymorphic sites and differences in N-linked glycosylation, the three-dimensional structure of rhLF closely matches the structure of natural hLF. This observation confirms earlier findings of identical biochemical activity of hLF from

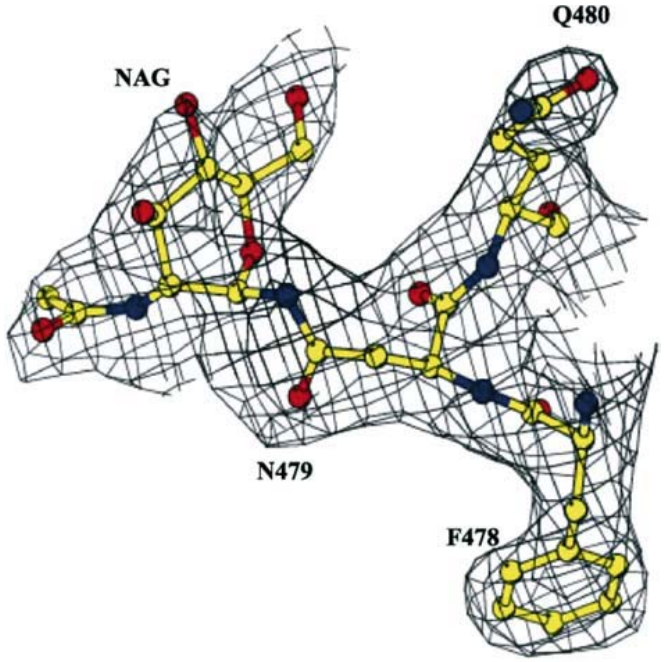

Figure 5. Crystallographic electron density surrounding Asn^{479}. Amino acid residues Phe^{478}, Asn^{479}, and Gln^{480} and *N*-acetylglucosamine (NAG) are shown in ball-and-stick representation surrounded by the final $2F_o–F_c$ electron density map contoured at 0.9σ. Picture was prepared with BOBSCRIPT (Esnouf, 1999), which is based on MOLSCRIPT (Kraulis, 1991).

both sources, paving the way for safe usage of rhLF in humans. In addition, the results illustrate the potential of transgenic cows to produce recombinant human proteins with a virtually identical structure compared to their human counterparts.

Acknowledgments

We thank R.A.G. de Graaff, N.S. Pannu and M.L. Mannesse for helpful discussions.

References

Anderson BF, Baker HM, Norris GE, Rice DW and Baker EN (1989) Structure of human lactoferrin: Crystallographic structure analysis and refinement at 2.8 Å. resolution. *J Mol. Biol* **209**: 711–734.

Appelmelk BJ, An YQ, Geerts M, Thijs BG, de Boer HA, MacLaren DM, de Graaff J and Nuijens JH (1994) Lactoferrin is a lipid A-binding protein. *Infect Immun* **62**: 2628–2632.

Baker HM, Anderson BF, Kidd RD, Shewry SC and Baker EN (2000) Lactoferrin three-dimensional structure: a framework for interpreting function. In: Shimazaki K (ed), Lactoferrin: Structure, Function and Applications (pp. 3–15) Elsevier Science, Amsterdam.

Collaborative Computational Project Number 4 (1994). The CCP4 suite: programs for protein crystallography. *Acta Cryst* **D50**: 760–763.

DeLano WL (2002) The PyMOL Molecular Graphics System on World Wide Web http://www.pymol.org.

Ellison III RT and Giehl TJ (1991) Killing of gram-negative bacteria by lactoferrin and lysozyme. *J Clin Invest* **88**: 1080–1091.

Ellison III RT, Giehl TJ and La FF (1988) Damage of the outer membrane of enteric gram-negative bacteria by lactoferrin and transferrin. *Infect Immun* **56**: 2774–2781.

Esnouf RM (1999) Further additions to MolScript version 1.4, including reading and contouring of electron-density maps. *Acta Cryst* **D55**: 938–940.

Evans PR (1993) Data collection and processing. In: Dodson E, Moore M, Ralph A and Bailey S (eds), *Proceedings of the CCP4 study weekend 1993* (pp. 114–122) CLRC Daresbury, Warrington.

Haridas M, Anderson BF and Baker EN (1995) Structure of human diferric lactoferrin refined at 2.2 Å resolution. *Acta Cryst* **D51**: 629–646.

He J and Furmanski P (1995) Sequence specificity and transcriptional activation in the binding of lactoferrin to DNA. *Nature* **373**: 721–724.

Hutchens TW and Yip TT (1991) Metal ligand-induced alterations in the surface structures of lactoferrin and transferrin probed by interaction with immobilized copper(II) ions. *J Chromatogr* **536**: 1–15.

Kijlstra A and Jeurissen SHM (1982) Modulation of the classical C3 convertase of complement by tear lactoferrin. *Immunology* **47**: 263–270.

Kraulis PJ (1991) MOLSCRIPT: A program to produce both detailed and schematic plots of protein structures. *J Appl Crystallog* **24**: 946–950.

Lamzin VS and Wilson KS (1997) Automated refinement for protein crystallography. *Methods Enzymol* **277**: 269-305.

Laskowski RA, MacArthur MW, Moss DS and Thornton JM (1993) PROCHECK: A program to check the stereochemical quality of protein structures. *J Appl Cryst* **26**: 283–291.

Lee WJ, Farmer JL, Hilty M and Kim YB (1998) The protective effects of lactoferrin feeding against endotoxin lethal shock in germfree piglets. *Infect Immun* **66**: 1421–1426.

Legrand D, van Berkel PHC, Salmon V, van Veen HA, Slomianny MC, Nuijens JH and Spik G (1997) The N-terminal Arg2, Arg3 and Arg4 of human lactoferrin interact with sulphated molecules but not with the receptor present on Jurkat human lymphoblastic T-cells. *Biochem J* **327**: 841–846.

Leslie AG (1999) Integration of macromolecular diffraction data. *Acta Cryst* **D55**: 1696–1702.

Mann DM, Romm E and Migliorini M (1994) Delineation of the glycosaminoglycan-binding site in the human inflammatory response protein lactoferrin. *J Biol Chem* **269**: 23661–23667.

McRee DE (1999) XtalView/Xfit – A versatile program for manipulating atomic coordinates and electron density. *J Struct Biol* **125**: 156–165.

Metz-Boutigue M, Jolles J, Mazurier J, Schoentgen F, Legrand D, Spik G, Montreuil J and Jolles P (1984) Human lactotransferrin: Amino acid sequence and structural comparisons with other transferrins. *Eur J Biochem* **145**: 659–676.

Murshudov GN, Vagin AA and Dodson EJ (1997) Refinement of macromolecular structures by the maximum-likelihood method. *Acta Cryst* **D53**: 240–255.

Nagasako Y, Saito H, Tamura Y, Shimamura S and Tomita M (1993) Iron-binding properties of bovine lactoferrin in iron-rich solution. *J Dairy Sci* **76**: 1876–1881.

Nuijens JH, van Berkel PHC and Schanbacher FL (1996) Structure and biological actions of lactoferrin. *J Mammary Gland Biol Neoplasia* **1**: 285–295.

Reiter B, Brock JH and Steel ED (1975) Inhibition of *Eschericia coli* by bovine colostrum and post-colostral milk II: The bacteriostatic effect of lactoferrin on a serum-susceptible and serum-resistant strain of *E. coli*. *Immunol* **28**: 83–95.

Rey MW, Woloshuk SL, de Boer HA and Pieper FR (1990) Complete nucleotide sequence of human mammary gland lactoferrin. *Nucleic Acids Res* **18**: 5288.

Sanchez L, Calvo M and Brock JH (1992) Biological role of lactoferrin. *Arch Dis Child* **67**: 657–661.

Spik G, Strecker G, Fournet B, Bouquelet S, Montreuil J, Dorland L, Van Halbeek H and Vliegenthart JFG (1982) Primary structure of the glycans from human lactotransferrin. *Eur J Biochem* **121**: 413–419.

Sun X-L, Baker HM, Shewry SC, Jameson GB and Baker EN (1999) Structure of recombinant human lactoferrin expressed in Aspergillus awamori. *Acta Cryst* **D55**: 403–407.

Vagin A and Teplyakov A (1997) MOLREP: An automated program for molecular replacement. *J Appl Cryst* **30**: 1022–1025.

van Berkel PH, van Veen HA, Geerts ME, de Boer HA and Nuijens JH (1996) Heterogeneity in utilization of N-glycosylation sites Asn624 and Asn138 in human lactoferrin: A study with glycosylation-site mutants. *Biochem J* **319**: 117–122.

van Berkel PHC, Geerts MEJ, van Veen HA, Kooiman PM, Pieper F, de Boer HA and Nuijens JH (1995) Glycosylated and unglycosylated human lactoferrins can both bind iron and have identical affinities towards human lysozyme and bacterial lipopolysaccharide, but differ in their susceptibility towards tryptic proteolysis. *Biochem J* **312**: 107–114.

van Berkel PHC, Welling MM, Geerts M, van Veen HA, Ravensbergen B, Salaheddine M, Pauwels EKJ, Pieper F, Nuijens JH and Nibbering PH (2002) Large scale production of recombinant human lactoferrin in the milk of transgenic cows. *Nat Biotechnol* **20**: 484–487.

van Veen HA, Geerts MEJ, van Berkel PHC and Nuijens JH (2004) The role of N-linked glycosylation in the protection of human and bovine lactoferrin against tryptic proteolysis. *Eur J Biochem* **271**: 678–684.

Vriend G (1990) WHAT IF: A molecular modeling and drug design program. *J Mol Graph* **8**: 52–56.

Ziere GJ, Bijsterbosch MK and van Berkel TJ (1993) Removal of 14 N-terminal amino acids of lactoferrin enhances its affinity for parenchymal liver cells and potentiates the inhibition of beta-very low density lipoprotein binding. *J Biol Chem* **268**: 27069–27075.

Zucali JR, Broxmeyer HE, Levy D and Morse C (1989) Lactoferrin decreases monocyte-induced fibroblast production of myeloid colony-stimulating activity by suppressing monocyte release of interleukin-1. *Blood* **74**: 1531–1536.